

Potential of systems subjected to weak noise with large correlation time

Hu Gang and Lu Zhi-heng

Center of Theoretical Physics, Chinese Center of Advanced Science and Technology (World Laboratory),

P.O.B. 8730, Beijing, China

*and Department of Physics, Beijing Normal University, Beijing, China**

(Received 10 October 1990; revised manuscript received 12 March 1991)

Colored-noise-driven bistable systems are considered in the weak-noise limit $D \rightarrow 0$ and long-correlation-time limit $\tau \rightarrow \infty$. The analytic solution of the two-dimensional Fokker-Planck equation is worked out. The theoretical result is compared with a numerical simulation.

PACS number(s): 05.40.+j, 05.20.-y

I. INTRODUCTION

A problem of great interest in nonequilibrium statistical physics is to investigate the behavior of systems subjected to colored noise [1–13]. Due to the nonzero correlation time of noise, the system may have essentially new features, which cannot be observed in white-noise cases. A number of physically interesting and mathematically hard problems remains to be answered. Among them, the most challenging one is the so-called negative-diffusion problem [6–8].

Let us consider a Langevin equation

$$\dot{X} = aX - X^3 + Q(t), \quad (1.1)$$

$$\langle Q(t) \rangle = 0,$$

$$\langle Q(t)Q(s) \rangle = \frac{D}{\tau} \exp\left[-\frac{|t-s|}{\tau}\right]. \quad (1.2)$$

At finite correlation time τ , (1.1) is non-Markovian. However, it can be reformulated as Markovian equations in two-dimensional space

$$\begin{aligned} \dot{X} &= aX - X^3 + Y, \\ \dot{Y} &= -Y/\tau + \Gamma(t), \end{aligned} \quad (1.3)$$

$$\langle \Gamma(t) \rangle = 0,$$

$$\langle \Gamma(t)\Gamma(s) \rangle = \frac{2D}{\tau^2} \delta(t-s), \quad (1.4)$$

which is equivalent to a two-dimensional Fokker-Planck equation (FPE)

$$\begin{aligned} \frac{\partial P(X, Y, t)}{\partial t} &= -\frac{\partial}{\partial X} [(aX - X^3 + Y)P] \\ &+ \frac{\partial}{\partial Y} \left[\frac{Y}{\tau} P \right] + \mathcal{E} \frac{\partial^2 P}{\partial Y^2} \\ \mathcal{E} &= D/\tau^2. \end{aligned} \quad (1.5)$$

The prevailing approach in dealing with (1.5) is to project into one-dimensional space and to truncate the resulting equation to an effective one-dimensional FPE. It has been shown that, as

$$\tau > 1/a, \quad (1.6)$$

a negative diffusion coefficient arises that may cause a conceptual problem of negative probability distribution. Faetti [10], Tsironis [11], and Hanggi [12] and their co-workers have suggested various approaches to overcome the difficulty. However, no reasonable result about the probability distribution in the unstable region $|x| < \sqrt{a}/3$ has been obtained.

In Ref. [14] we suggested a steepest-descent approximation in solving (1.5) in the weak-noise limit

$$D \ll 1, \quad (1.7)$$

where we expanded the stationary solution of (1.5) as

$$\begin{aligned} P(X, Y) \\ = N \exp[-\phi_0(X, Y)/D - \phi_1(X, Y) - D\phi_2(X, Y) - \dots] \end{aligned} \quad (1.8)$$

and identified the valley of the potential, i.e., $\phi_0(X, Y)$, to the curve

$$Y + aX - X^3 = 0. \quad (1.9)$$

Since the weak-noise limit $D \rightarrow 0$ is taken, we will consider only the potential $\phi_0(X, Y)$ in the probability distribution (1.8) afterwards.

Equation (1.5) does not obey the detailed balance condition [5–7]. Consequently, an analytic solution of (1.5) cannot be provided. Thus, numerical simulation on Eq. (1.5) for small D and large τ is extremely important in verifying and comparing various approximations. Nevertheless, the difficulty of numerical work increases rapidly as D decreases. To date, no numerical result has been obtained which can really represent the behavior of the solution of (1.5) in the limits $D \rightarrow 0$, $\tau \rightarrow \infty$.

The weak-noise limit $D \rightarrow 0$ should be regarded as one of the most important limits in treating the FPE's like (1.5) [15]. On the one hand, this limit well meets a practical situation where noise due to microscopic reasons is considerably smaller than macroscopic variables. On the other hand, the weak-noise limit may considerably reduce the difficulty in computing the equation and obtaining analytic results. The central task of the present paper is to

get an analytic solution of FPE (1.5) in the weak-noise limit $D \rightarrow 0$ and in the limit $\tau \rightarrow \infty$.

Inserting (1.8) into (1.5) and keeping only the leading terms of D we obtain the Hamilton-Jacobi equation [16–24]

$$[Y + f(X)] \frac{\partial \phi_0}{\partial X} - \frac{Y}{\tau} \frac{\partial \phi_0}{\partial Y} + \left[\frac{\partial \phi_0}{\partial Y} \right]^2 / \tau^2 = 0, \tag{1.10}$$

$$f(X) = aX - X^3.$$

A well-known property of the potential is that $\phi_0(X, Y)$ is a Lyapunov function of the corresponding deterministic equations

$$\begin{aligned} \frac{d\phi_0(X, Y)}{dt} &= \frac{\partial \phi_0}{\partial X} \dot{X} + \frac{\partial \phi_0}{\partial Y} \dot{Y} \\ &= \frac{\partial \phi_0}{\partial X} C_1(X, Y) + \frac{\partial \phi_0}{\partial Y} C_2(X, Y) \\ &= - \left[\frac{\partial \phi_0}{\partial Y} \right]^2 / \tau^2 \leq 0, \end{aligned} \tag{1.11}$$

where we use

$$\begin{aligned} \dot{X} &= C_1(X, Y), \\ \dot{Y} &= C_2(X, Y), \end{aligned} \tag{1.12a}$$

$$C_1(X, Y) = Y + aX - X^3, \quad C_2(X, Y) = -\frac{Y}{\tau}. \tag{1.12b}$$

The third equality of (1.11) is due to the Hamilton-Jacobi equation (1.10). Hence, $\phi_0(X, Y)$ must not increase along the deterministic trajectory.

In Ref. [25], we suggested an expansion of the potential around the potential valley (1.9),

$$\begin{aligned} \phi_0(X, Y) &= \phi_0(X) + \phi_2(X)Y^2 + \dots, \\ V = Y + f(X) &= Y + aX - X^3, \end{aligned} \tag{1.13}$$

and obtained an iterative equation for $\phi_i(X)$ as

$$\phi_0(X) = -\frac{2}{\tau} \int f(X)\phi_2(X)dX, \tag{1.14a}$$

$$-2 \left[\frac{1}{\tau} - f'(X) \right] \phi_2(X) + \frac{3}{\tau} f\phi_3(X) + 4\phi_2^2(X)/\tau^2 = 0, \tag{1.14b}$$

$$-3 \left[\frac{1}{\tau} - f'(X) \right] \phi_3(X) + \phi_2'(X) + \frac{4}{\tau} f(X)\phi_4(X) + 12\phi_2(X)\phi_3(X)/\tau^2 = 0, \tag{1.14c}$$

... ..

$$-n \left[\frac{1}{\tau} - f'(X) \right] \phi_n(X) + \phi_{n-1}'(X) + \frac{n}{\tau} f(X)\phi_{n+1}(X) + \sum_{k=3}^{n-1} k(n+2-k)\phi_k(X)\phi_{n+2-k}(X)/\tau^2 = 0, \tag{1.14d}$$

from which $\phi_i(X)$ can be obtained successively.

In Sec. II, we apply (1.14) to some solvable models and obtain exact solutions. The structure of the two-dimensional probability distribution in the limit $D \rightarrow 0$, $\tau \rightarrow \infty$ is analyzed. Section III is devoted to solving (1.14) and obtaining the analytic form of the potential of bistable systems in the limit $\tau \rightarrow \infty$. A comparison of our analytic result with those of the previous theories and with a numerical simulation will also be presented in Sec. III.

II. EXACTLY SOLVABLE MODELS

In order to show the validity of the iterations (1.14) and to get intuitive ideals about the structure of the potential in the limit $\tau \rightarrow \infty$, we analyze certain solvable models. The first model is the following FPE:

$$\frac{\partial P(X, Y, t)}{\partial t} = \frac{\partial}{\partial X} [(aX - Y)P] + \frac{\partial}{\partial Y} \left[\frac{Y}{\tau} P \right] + \mathcal{E} \frac{\partial^2 P}{\partial Y^2}, \tag{2.1}$$

which leads to the Hamilton-Jacobi equation (1.10) with $f(X)$ being replaced by

$$f(X) = -aX, \quad a > 0. \tag{2.2}$$

Inserting (2.2) into (1.14), we obtain

$$\phi_2(X) = \frac{\tau}{2} [1 + a\tau], \tag{2.3a}$$

$$\phi_0(X) = \frac{a(1+a\tau)}{2} X^2, \tag{2.3b}$$

$$\phi_3(X) = \phi_4(X) = \dots = \phi_n(X) = \dots = 0. \tag{2.3c}$$

Finally, we have

$$\phi_0(X, Y) = \frac{a(1+a\tau)}{2} X^2 + \frac{\tau(1+a\tau)}{2} (Y - aX)^2. \tag{2.4a}$$

Actually, the probability distribution

$$P(X, Y) = N \exp[-\phi_0(X, Y)/D] \tag{2.4b}$$

with $\phi_0(X, Y)$ given by (2.4a) is the exact stationary solution of (2.1).

It is obvious that the curve

$$Y = -f(X) = aX \tag{2.5}$$

is the potential valley with respect to Y ; that is consistent with our argument in Refs. [14] and [25]. It is worthwhile remarking that, in the limit $\tau \rightarrow \infty$, there exist two characteristic directions in the potential profile. Along the potential valley (2.5), $\phi_0(X, Y)$ is proportional to τ ,

$$\phi_0(X, Y = aX) \approx \frac{a^2 \tau}{2} X^2, \tag{2.6}$$

while along the direction perpendicular to the potential valley, $\phi_0(X, Y)$ increases rapidly as

$$\phi_0(X, Y = -X/a) \approx \frac{a(a^2 + 1)\tau^2}{2} \Delta s^2, \tag{2.7}$$

where Δs is the distance between the given point and the potential valley. The existence of the two distinctive scal-

ing directions of the potential in the limit $\tau \rightarrow \infty$ will be shown to be very important for understanding the structure of the potential of a more complicated system (1.5).

For the second model, we study a nonlinear though single-basin system

$$f(X) = -aX - X^3, \quad a > 0. \tag{2.8}$$

Now the deterministic equations (1.12) have a unique attracting center, the origin (0.0). In the limit $\tau \rightarrow \infty$, $\phi_n(X)$ in Eqs. (1.14) are decoupled from all the upper terms $\phi_m(X)$, $m > n$, and then can be exactly solved successively from below. For instance, we have

$$\phi_2(X) = \frac{\tau}{2} [1 + \tau f'(X)], \tag{2.9a}$$

$$\phi_0(X) = \int f(X) dX + \frac{\tau^2}{2} f(X)^2. \tag{2.9b}$$

Integrating $P(X, Y) = N \exp[-\phi_0(X, Y)/D]$ over Y and considering $D \rightarrow 0$, we have

$$P(X) = NG(X) \exp \left[- \left(\frac{aX^2}{2} + \frac{1}{4} X^4 \right) / D - \frac{\tau}{2} (aX + X^3)^2 / D \right], \tag{2.10}$$

where $G(X)$ is a D -independent function. Apart from the prefactor, Eq. (2.10) is the exact stationary probability distribution of X in the weak-noise limit $D \rightarrow 0$ and in the long correlation time limit $\tau \rightarrow \infty$. The D -independent prefactor is negligibly smaller than that of the potential and will be ignored from our consideration. Thus, Eq. (2.10), which is reduced from the two-dimensional probability distribution (1.8), (1.13), and (2.9), is identical to the exact solution obtained from the effective Fokker-Planck equations [19,20,26,27]. We would like to emphasize that Eqs. (2.9) and (1.13) contain more information than (2.10). From (2.9), we know the potential in two-dimensional space. This knowledge turns out to be extremely important as multibasin systems are considered. With (2.9a) and (2.9b), we find again two characteristic directions of $\phi_0(X, Y)$. Along the potential valley

$$Y = aX + X^3, \tag{2.11}$$

the potential increases from the origin in the manner

$$\phi_0(X, Y = aX + X^3) \approx C_1 \tau, \tag{2.12a}$$

where C_1 is a τ -independent function of X . In the perpendicular direction, the potential increases much more rapidly as

$$\phi_0(X, Y) \approx C_2 \tau^2 \Delta s^2, \tag{2.12b}$$

where C_2 is again a τ -independent function of X and Δs is the distance between the given point and the potential valley. Hence, the variation of the potential along the potential valley is infinitely slower than that along the perpendicular direction.

III. THE POTENTIAL OF DOUBLE-BASIN SYSTEM

In this section, we come to our main problem, the study of the potential of bistable systems. An analysis of the trajectory of the corresponding deterministic equations (1.12) is particularly useful for understanding the peculiar structure of the potential (see Ref. [12]). In Fig. 1, we plot the deterministic flow in the limit $\tau \rightarrow \infty$. The arrows denote the directions of the trajectories. The dotted line represents the curve

$$Y = -aX + X^3. \tag{3.1}$$

The turning points A and B are located at

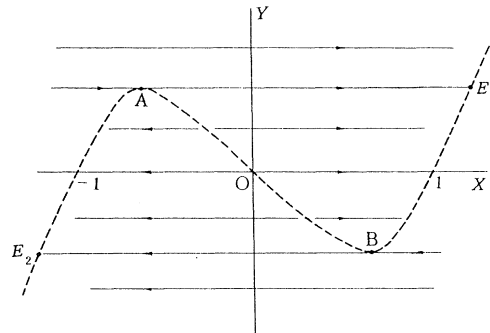


FIG. 1. The deterministic paths of Eqs. (1.12) in the limit $\tau \rightarrow \infty$, $a = 1$. The arrows indicate the directions of the trajectories. The dashed line is plotted according to $Y + X - X^3 = 0$. The system approaches the segments AE_2 and BE_1 while it runs away from AOB .

$$\begin{aligned}
 X_{A,B} &= \mp \sqrt{a/3}, \\
 Y_{A,B} &= \pm \frac{2a}{3} \sqrt{a/3},
 \end{aligned}
 \tag{3.2}$$

respectively.

It is reasonable to take the potential (2.9) [note, now the function $f(X)$ in (2.9) should be $aX - X^3$ rather than (2.8); this fact is understood afterwards] as the correct expression of the stationary solution in the region

$$|X| > \sqrt{a/3} . \tag{3.3}$$

The validity of (2.9) can be verified by integrating the resulting stationary solution over Y that leads to

$$\begin{aligned}
 P(X) &= NH(X) \\
 &\times \exp \left[\left(\frac{aX^2}{2} - \frac{1}{4}X^4 \right) / D - \frac{\tau}{2} (aX - X^3)^2 / D \right]
 \end{aligned}
 \tag{3.4}$$

with $H(X)$ being independent of D . Equation (3.4) is the well-known exact solution of (1.5) in the limits $D \rightarrow 0$, $\tau \rightarrow \infty$ in the region (3.3) [11,23,27]. In the region

$$|X| < \sqrt{a/3}, \tag{3.5}$$

(2.9) [or equivalently, (3.4)] is no longer the solution of (1.5) in the limits $D \rightarrow 0$, $\tau \rightarrow \infty$. Nevertheless, the probability distribution in the unstable region (3.5) can be computed as follows.

First, we can use (2.9) to calculate the potential at A . Inserting (3.2) into (2.9) and (1.13), we have

$$\phi_0(X_A, Y_A) = 2a^3\tau/27 . \tag{3.6}$$

In Ref. [12], it is argued that the probability density at A (and B) is the maximum on the barrier between the two basins. In other words, the potential at A (and B) is the lowest on the separatrix of the two attractors. Therefore, the probability transition between the two wells must take place in the vicinity of A (and B). Since the drift at A is infinitely small, a small random force can easily spread probability apart from this point. Hence, slightly above or right to A , the probability density must be of order (3.6). Above A , the system is mainly evolved by the deterministic dynamics [11,28,29]. Thus, the probability transition in the bistable system takes place mainly through the channels AE_1 (from left to right) and BE_2 (from right to left) which are parallel to the X axis. Since the time needed for probability to flow from A to the right basin (or from B to the left basin) is finite and the probability flow is steady, the probability density on all the channels AE_1 (and on BE_2) must be of order (3.6). This conclusion is consistent with the solution (3.4), according to which the potentials at A, B, E_1 and E_2 are all equal to (3.6) in the limit $\tau \rightarrow \infty$. From Eqs. (1.5) and (2.9), the width of the channel can be estimated to be of the order $1/\tau$.

From the previous analysis, the stationary probability distribution in the X - Y plane, in the limits $D \rightarrow 0$, $\tau \rightarrow \infty$, becomes clear. The essentially new results on the station-

ary probability distribution can be described as follows.

(1) In the region (3.3), there are two potential valleys AE_2 and BE_1 , along which the potential is correctly represented by the analytic formula (2.9). In the unstable region (3.5), there are also two potential valleys AE_1 and BE_2 on which the potential is identical to that at A and B . Outside or inside the closed curve E_2AE_1B , the potential increases so rapidly that the probability away from this circle can be neglected.

(2) In the region (3.5), the probability on the two channels AE_1 and BE_2 has highest density. Therefore, the absolutely major part of probability transition between the two basins takes place through these channels.

(3) Since the probability density inside the circle AE_1BE_2 is much lower than that on the circle, it is reasonable to expect a probability hole at the origin. This conclusion is identical to the numerical observations [30–32].

(4) The probability density at A and B is given in Eq. (3.6). In the weak-noise and large correlation time limits, the potential on the channels AE_1 and BE_2 is also given by (3.6). According to argument (1), the reduced probability density $P(X) = \int P(X, Y)dY$ can be explicitly given by

$$\lim_{\substack{D \rightarrow 0 \\ \tau \rightarrow \infty}} (D/\tau) \ln P(X) = \begin{cases} \frac{-(aX - X^3)^2}{2}, & |X| > \sqrt{a/3}, \\ -2a^3/27, & |X| < \sqrt{a/3}. \end{cases} \tag{3.7}$$

Equation (3.7) is a good approximation of the one-dimensional stationary probability distribution for small D and large τ . In the limits $D \rightarrow 0$ and $\tau \rightarrow \infty$, the result becomes exact. We would like to emphasize that the analytic form (3.7) essentially improves the expression in Ref. [10] where the probability in the unstable region (3.5) is assumed to be zero.

The probability distribution (3.7) leads to a mean first passage time

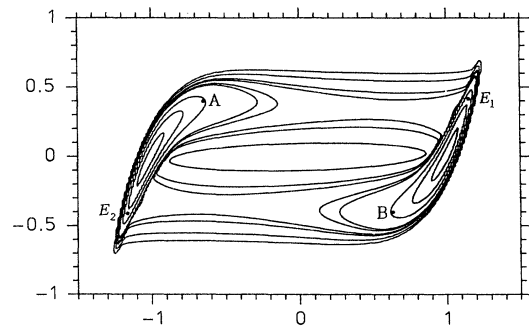


FIG. 2. The numerical level curves of the stationary solution of the FPE (1.5). $D = 0.01$, $\tau = 10$, and $a = 1$. The points A, B, E_1 , and E_2 are the same as those indicated in Fig. 1. In the unstable region (3.5) there are two probability density humps on AE_1 and BE_2 on which the level curves are rather rare and the potential there is practically uniform. A probability hole exists around the origin.

$$T \propto \exp(2a^3\tau/27D)$$

which is consistent with the result in Refs. [11], [12], and [33–35].

To verify the above theoretical prediction, we numerically solve the FPE (1.5). To our knowledge, numerical simulation of (1.5) for small D and large τ is still lacked to date, and then it is interesting by itself to accomplish this task. A finite-difference method with a Grank-Nicolson implicit mode is used to simulate Eq. (1.5). To avoid the divergence in the weak-noise case, we use the upstream scheme instead of the central difference scheme. A detailed report about this matter will appear elsewhere [32]. Here we only present the result of one of the simulations. In Fig. 2, we fix D , τ , and a to 0.01, 10, and 1, respectively, and plot the level curves of the stationary probability density. The following features are obvious in the figure.

(1) In the region $|X| > \sqrt{1/3}$, there are two potential

valleys (i.e., two probability density humps) along AE_2 and BE_1 (to compare with Fig. 1) vertical to which the level curves are rather dense.

(2) There are two other potential valleys in the region $|X| < \sqrt{1/3}$ along AE_1 and BE_2 on which the level curves are very rare. The potential on these valleys is practically uniform.

(3) A probability hole occurs at the origin, the deterministic saddle point.

All these features, which are observed in all numerical simulations of Eq. (1.5) with small D and large τ [32], are completely consistent with the above theoretical predictions.

ACKNOWLEDGMENT

This work is supported by the Nature Science Foundation of China.

*Address to which correspondence should be sent.

- [1] R. L. Stratnovich, *Topics in the Theory of Random Noise* (Gordon and Breach, New York, 1967), Vol. I.
- [2] P. Hanggi, F. Marchesoni, and P. Grigolini, *Z. Phys. B* **56**, 333 (1984).
- [3] P. Hanggi, T. J. Mroczkowski, F. Moss, and P. V. E. McClintock, *Phys. Rev. A* **32**, 695 (1985).
- [4] R. F. Fox, *Phys. Rev. A* **37**, 911 (1988).
- [5] T. Leiber, F. Marchesoni, and H. Risken, *Phys. Rev. A* **38**, 983 (1988).
- [6] J. M. Sancho, F. Sagues, and M. San Miguel, *Phys. Rev. A* **33**, 3399 (1986).
- [7] J. Masoliver, B. J. West, and K. Lindenberg, *Phys. Rev. A* **35**, 3086 (1987).
- [8] R. F. Fox, *Phys. Rev. A* **33**, 467 (1986); **34**, 4525 (1986).
- [9] R. F. Fox, *Phys. Rev. A* **37**, 911 (1988).
- [10] S. Faetti, L. Fronzoni, P. Grigolini, and R. Mannella, *J. Stat. Phys.* (to be published).
- [11] G. P. Tsironis and P. Grigolini, *Phys. Rev. A* **38**, 3749 (1988).
- [12] P. Hanggi, P. Jung, and F. Marchesoni, *J. Stat. Phys.* **54**, 1367 (1989).
- [13] P. Grigolini, L. A. Lugiato, R. Mannella, P. V. McClintock, M. Merri, and M. Pernigo, *Phys. Rev. A* **38**, 1966 (1988).
- [14] G. Hu and H. Haken, *Phys. Rev. A* **41**, 7078 (1990).
- [15] H. Risken, *The Fokker-Planck Equation* (Springer, New York, 1983).
- [16] R. Graham and A. Schenzle, *Z. Phys. B* **52**, 61 (1983).
- [17] R. Graham, D. Roekaerts, and T. Tel, *Phys. Rev. A* **31**, 3364 (1985).
- [18] R. Graham and T. Tel, *Phys. Rev. A* **33**, 1322 (1986).
- [19] P. Colet, H. S. Wio, and M. S. Miguel, *Phys. Rev. A* **39**, 6094 (1989).
- [20] H. S. Wio, P. Colet, and M. S. Miguel, *Phys. Rev. A* **40**, 7312 (1989).
- [21] A. J. Bray and A. J. McKane, *Phys. Rev. Lett.* **62**, 593 (1989).
- [22] A. Schenzle and T. Tel, *Phys. Rev. A* **32**, 596 (1985).
- [23] G. Hu, *Phys. Rev. A* **38**, 3693 (1988).
- [24] G. Hu and H. Haken, *Phys. Rev. A* **40**, 5966 (1989).
- [25] G. Hu, *Phys. Rev. A* **43**, 700 (1991).
- [26] J. M. Sancho and M. S. Miguel, *Phys. Rev. A* **26**, 1589 (1982).
- [27] P. Jung and P. Hanggi, *Phys. Rev. A* **35**, 4464 (1987).
- [28] M. Suzuki, Y. Liu, and T. Tsuno, *Physica A* **38**, 433 (1986).
- [29] G. Hu and Q. Zheng, *Phys. Lett.* **110A**, 65 (1985).
- [30] F. Marchesoni and F. Moss, *Phys. Lett. A* **131**, 322 (1988).
- [31] G. Debnath, F. Moss, T. Leiber, H. Risken, and F. Marchesoni, *Phys. Rev. A* **42**, 703 (1990).
- [32] Z. H. Lu, L. Schoendorff, H. Risken, and G. Hu, *Chin. Phys. Lett.* (to be published).
- [33] A. Forster and A. S. Mikhailov, *Phys. Lett. A* **126**, 459 (1988).
- [34] J. F. Luciani and A. D. Verga, *Europhys. Lett.* **4**, 255 (1987).
- [35] J. F. Luciani and A. D. Verga, *J. Stat. Phys.* **50**, 567 (1988).